american physiological society

JOURNAL OF APPLIED PHYSIOLOGY

J Appl Physiol 134: 957–968, 2023.
First published February 9, 2023; doi:10.1152/japplphysiol.00591.2022

RESEARCH ARTICLE

Inhibition of knee joint sensory afferents alters covariation across strides between quadriceps muscles during locomotion

Cristiano Alessandro,[1,2] Adarsh Prashara,[3] David P. Tentler,[1] and Matthew C. Tresch[1,3,4,5]

[1]*Department of Neuroscience, Northwestern University, Chicago, Illinois, United States;* [2]*School of Medicine and Surgery/Sport and Exercise Medicine, University of Milano-Bicocca, Milan, Italy;* [3]*Department of Biomedical Engineering, Northwestern University, Evanston, Illinois, United States;* [4]*Department of Physical Medicine and Rehabilitation, Northwestern University, Chicago, Illinois, United States; and* [5]*Shirley Ryan AbilityLab, Chicago, Illinois, United States*

Abstract

Sport-related injuries to articular structures often alter the sensory information conveyed by joint structures to the nervous system. However, the role of joint sensory afferents in motor control is still unclear. Here, we evaluate the role of knee joint sensory afferents in the control of quadriceps muscles, hypothesizing that such sensory information modulates control strategies that limit patellofemoreal joint loading. We compared locomotor kinematics and muscle activity before and after inhibition of knee sensory afferents by injection of lidocaine into the knee capsule of rats. We evaluated whether this inhibition reduced the strength of correlation between the activity of vastus medialis (VM) and vastus lateralis (VL) both across strides and within each stride, coordination patterns that limit net mediolateral patellofemoral forces. We also evaluated whether this inhibition altered correlations among the other quadriceps muscle activity, the time-profiles of individual EMG envelopes, or movement kinematics. Neither the EMG envelopes nor limb kinematics was affected by the inhibition of knee sensory afferents. This perturbation also did not affect the correlations between VM and VL, suggesting that the regulation of patellofemoral joint loading is mediated by different mechanisms. However, inhibition of knee sensory afferents caused a significant reduction in the correlation between vastus intermedius (VI) and both VM and VL across, but not within, strides. Knee joint sensory afferents may therefore modulate the coordination between the vasti muscles but only at coarse time scales. Injuries compromising joint afferents might result in altered muscle coordination, potentially leading to persistent internal joint stresses and strains.

NEW & NOTEWORTHY Sensory afferents originating from knee joint receptors provide the nervous system with information about the internal state of the joint. In this study, we show that these sensory signals are used to modulate the covariations among the activity of a subset of vasti muscles across strides of locomotion. Sport-related injuries that damage joint receptors may therefore compromise these mechanisms of muscle coordination, potentially leading to persistent internal joint stresses and strains.

feedback control; internal joint loading; locomotion; muscle coordination; sensory inhibition

INTRODUCTION

The central nervous system (CNS) receives rich sensory information from a variety of receptors across the body. This information is used extensively to generate appropriate motor commands during movement execution (1). Sensory receptors within muscles convey information about muscle length, velocity, and tension, mediating fast reflex loops in the spinal cord (1) as well as allowing the estimation of body posture and state in higher neural structures (2). The interruption of these afferent pathways, potentially due to neuropathies (3) or injuries (4), causes substantial impairment to movement execution (5, 6) and to musculoskeletal function (7, 8).

Sensory information, however, also originates from receptors within joint structures, such as ligaments, the menisci in the knee, and the joint capsule (9). These joint sensory afferents can carry information about stresses and strains within the joint (10). Thus, they may be involved in neural circuitry to maintain joint stability (11) and to limit joint loading (12–14). Since internal joint stresses and strains also depend on body posture, joint sensory afferents may also be used by the CNS to estimate the posture of the body or external forces during movements, thereby facilitating task performance. According to these views, some previous studies showed that inhibition of joint sensory afferents causes significant short-term changes in movement execution (15) as well as the development of long-term joint conditions such as osteoarthritis (16, 17). However, other studies found that inhibition of joint sensory afferents causes no alterations in muscle activity during movement execution (18, 19). Although joint sensory

Correspondence: C. Alessandro (cristiano.alessandro@unimib.it).
Submitted 5 October 2022 / Revised 3 January 2023 / Accepted 6 February 2023

afferents affect the neural activity in both spinal and supraspinal circuitries (20), how the CNS uses this sensory information for either regulation of internal joint integrity or for task performance, therefore, remains unclear.

We re-examine these issues in the present study, evaluating the potential role of joint sensory afferents in the regulation of joint loading and the execution of movements. We take advantage of our recent work, which has identified signatures of neural control of joint stresses in the activation of quadriceps muscles during locomotion in the rat. That work showed that the electromyographic (EMG) activity of vastus medialis (VM) and vastus lateralis (VL) is highly correlated both across strides (i.e., the activation of each muscle integrated across the stance phase of locomotion covaried from one stride to the next) and within the gait cycle (i.e., the fine time course of muscles' activation covaried within each stride; 21). Such correlated activity of VM and VL is expected to minimize the net mediolateral force on the patella (22, 23) and therefore limit loading in the patellofemoral joint (24), in accordance with previous results on humans (24, 25). Activity in knee joint sensory afferents might be at least partially responsible for these correlations, conveying information about the internal state of the knee that may be used by the CNS to drive a coordinated activation of the quadriceps muscles. Furthermore, because of their slow dynamic responses (26), joint sensory afferents might only drive correlations at relatively course time scales, such as the across-stride correlations between integrated EMG activity, rather than driving correlations at fine time scales, such as the correlations between EMG time-varying profiles within single strides.

To evaluate these possibilities, we compare the strength of correlations between the activity of the quadriceps muscles before and after the inhibition of knee sensory afferents, obtained by injecting lidocaine into the knee capsule (Fig. 1). In addition, we evaluate the role of joint afferents in task performance, evaluating whether inhibition of knee joint afferents affects either limb kinematics or the time course of the EMG envelopes of each individual muscle during locomotion.

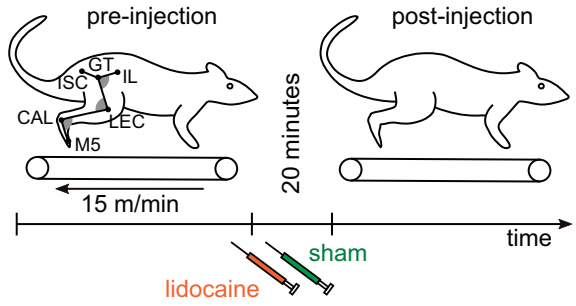

Figure 1. Experimental protocol. We compared movement kinematics and muscle activity during level locomotion before (pre) and 20 min after (post) the injection of lidocaine into the knee capsule to temporarily inhibit knee sensory afferents. For control, the same procedure was repeated by performing a sham injection that did not inhibit knee sensory afferents. The limb stick-figure is defined based on the anatomical placements of the markers: tuberosity of ischium (ISC), crest of ilium (IL), greater trochanter (GT), between the lateral epicondyle of the femur and the lateral condyle of the tibia (LEC), posterolateral extremity of calcaneus (CAL), lateral part of the 5th metatarsal bone (M5). Hip, knee, and ankle angles are defined as explained in METHODS.

METHODS

We performed experiments on adult female Sprague–Dawley rats (n = 12, weight = 0.30 ± 0.02 kg), some of which contributed also to another different study (21). All procedures were approved by the Animal Care Committee of Northwestern University.

Experimental Protocol

Rats were trained to maintain a stable walking gait during treadmill locomotion: i.e., maintaining a stable speed of walking without accelerations or decelerations that would bring the animals to the front or the back of the moving belt. We implanted chronic EMG electrodes in hindlimb muscles and allowed animals to recover for at least 10 days. We recorded movement kinematics and EMG activity of the left hindlimb (the only one visible by the motion tracking system) during level walking at 15 m/min, before and after the injection of lidocaine into the knee capsule. On a different day, the same experiment was repeated with a sham injection for control (see *Experimental Procedures*). The order of these experiments was randomized across rats to avoid biases. At the end of data collection, animals were euthanized and electrode location was verified (no misplaced electrodes were found). We also measured the electrical impedance of each electrode, and we excluded from the analysis electrodes with impedance higher than 50 kΩ (potentially indicating a damaged wire) and those with values close to zero (indicating a short circuit). Because of these criteria, we excluded the electrode associated to vastus intermedius (VI) in one animal.

Experimental Procedures

Before each recording session, we briefly anesthetized the animal under isoflurane (2%–3% in O_2 ~2 L/min) to attach the EMG connector in the rat to the amplifier via cable. We also secured retroreflective markers to the skin of the animal to measure hindlimb kinematics, as described previously (12). Markers were placed in the following anatomical locations identified by palpation (see Fig. 1*A*): tuberosity of ischium (ISC), crest of ilium (IL), greater trochanter (GT), between the lateral epicondyle of the femur and the lateral condyle of the tibia (LEC), posterolateral extremity of calcaneus (CAL), lateral part of the 5th metatarsal bone (M5). We then placed the animal on the treadmill, and waited at least 30 min before starting data collection to let the effect of isoflurane to wear off. We recorded at least 2 min of locomotion. After this baseline condition, the animal was lightly anesthetized (for less than 5 min) as described earlier, and either lidocaine or sham injection was performed. The skin overlying the knee joint capsule was shaved and disinfected, enabling visualization of the patellar tendon and joint capsule. A 31-G needle was carefully inserted within the knee capsule lateral to the patellar tendon, and either 0.05 mL of lidocaine or no solution (sham) was injected. The sham injection controlled for any effects of the additional isoflurane anesthesia or knee joint site preparation. Preliminary experiments with

injection of the same volume of colored dye confirmed that the injection filled without spreading outside the joint capsule.

Implantation of EMG Electrodes

The procedure to implant the EMG electrodes was described in detail previously (12, 13, 21). Briefly, we anesthetized animals with isoflurane (3% in O_2 ~2 L/min), shaved their hindlimb, and prepared them for aseptic surgery. We implanted pairs of electrodes in the quadriceps muscles: vastus lateralis (VL), vastus medialis (VM), rectus femoris (RF), and vastus intermedius (VI). Other muscles (up to 8 additional) were implanted in the same hindlimb but were not analyzed in this study. Knots placed on both sides of the muscle secured the exposed electrode sites within the muscle belly. The electrode leads were tunneled subcutaneously to a connector (Omnetics nano series) on the back of the animal. We implanted the deep muscle VI by separating the anterior head of biceps femoris from VL to expose the femur and gently lifting VL from the bone; VI was then clearly distinguishable from VL due to its distinct color and fiber organization. During the first 2 days after surgery, we administered analgesics (buprenorphine, 0.2 mg/kg, twice daily; meloxicam, 0.25 mg/kg, once daily).

Data Acquisition and Processing

Differential EMG signals were amplified (×1,000, A-M Systems Inc., Model 3500), band-pass (30–1,000 Hz) and notch filtered (60 Hz), and then digitized (5,000 Hz, Vicon Lock+, Model VL0143). The digitized signals were further high-pass filtered offline to remove motion artifacts (50 Hz, 4th-order Butterworth). To assess potential cross talk among EMG signals, we computed the cross-correlation between the unrectified activities of adjacent muscles. We discarded signals for which the absolute value of the peak cross-correlation was higher than 0.3 (27, 28). This only happened for one rat between muscles VL and VI. We rectified the remaining signals and computed their envelopes by low-pass filtering (20 Hz, 4th-order Butterworth).

The three-dimensional (3-D) position of markers was tracked using a motion capture system (Vicon Lock+, Model VL0143) at a frequency of 200 Hz. These signals were low-pass filtered offline at a cut-off frequency of 10 Hz (5th-order Butterworth). To reduce errors due to differential movements of the skin (29), we estimated the 3-D position of the knee by triangulation using the lengths of the femur and the tibia (29) in the plane defined by the markers on GT, LEC, and CAL. We then projected the 3-D positions of the markers and of the estimated knee in the sagittal plane, and computed the following joint angles (Fig. 1*A*): hip (angle between IL, GT, and estimated knee), knee (angle between GT, estimated knee, and CAL), and ankle (angle between estimated knee, CAL, and M5).

We segmented the EMG envelopes and the kinematic signals into separate strides, defining the beginning of each stride as the moment of foot-strike (i.e., when the foot touched the ground, as determined from the trajectory of the toe marker). To obtain consistent data for steady locomotion in each behavioral condition, we only considered strides with durations within 1.5 standard deviations from the mean duration; this criterion eliminated strides in which the animal either accelerated or decelerated across the treadmill. We also excluded strides with clear EMG artifacts that could occur when the cable hit the side of the treadmill, as identified using Tukey outlier analysis (i.e., identifying EMG values that were 1.5 interquartiles above the upper quartile of the maxima across steps). Application of these inclusion criteria resulted in data sets with an average of 175 strides (minimum of 30) for each animal and condition (pre/postinjection). These strides were time normalized for further analyses.

Measures of Muscle Activity and Correlation

We considered correlations between two measures of muscle activity: the overall activation intensity within each stride of locomotion, and the time-varying activation profiles within each gait cycle. The overall activation intensity of each muscle on each individual stride was calculated as the integral of the EMG envelope over the stance phase of locomotion [i.e., from foot-strike to foot-off, when all quadriceps muscles are consistently activated (30)], resulting in one numerical value for each muscle and stride. Note that this measure will be affected by the duration of the stance phase, with longer stance phases having larger integrated EMGs at a given value of mean EMG. We chose this measure as it was likely to best reflect the overall joint stress produced during an individual stride (i.e., longer stance phases at a given level of EMG likely produce more persistent joint loading) and so best reveal any potential role of joint afferents in regulating EMGs. We then calculated the Pearson correlation coefficients between the values of this measure of integrated EMG obtained for all strides, for each pair of quadriceps muscles (VM-VL, VM-VI, VL-VI, RF-VL, RF-VM, and RF-VI); we used these correlation coefficients as measures of muscle covariation across stride. We did this for each animal and experimental condition (i.e., pre/postinjection of lidocaine/sham). Thus, each animal contributed 24 correlation coefficients to subsequent analyses: six muscle pairs, at two time points relative to injection (pre- and postinjection), and for two types of injections (lidocaine and sham).

Changes in these correlation coefficients across conditions could be driven either by changes in the covariance between the integrated EMGs of pairs of muscles, or by changes in the variability of the integrated EMGs of each individual muscles across strides. These two possibilities were quantified as the numerator and denominator of the Pearson correlation coefficients ρ: $\rho_{m_1 m_2} = \frac{\mathrm{cov}(m_1,m_2)}{\sigma_{m_1}\sigma_{m_2}}$, where $\mathrm{cov}(m_1,m_2)$ indicates the across-stride covariation of the integrated EMGs of muscles m_1 and m_2, and σ_{m_1} and σ_{m_2} indicate the across-stride standard deviations of the integrated EMGs of muscles m_1 and m_2.

To evaluate the influence of knee joint sensory afferents on the covariations between the time-varying activation profile of quadriceps muscles within the gait cycle, we computed the Pearson correlation coefficient between the EMG envelopes of each pair of quadriceps muscles during the stance phase for each individual stride of locomotion. We then averaged these correlation coefficients across strides, for each muscle pair, experimental condition, and animal. These stride-averaged measures were then compared before and after lidocaine and sham injections.

To assess the influence of joint sensory afferents on the activity of individual muscles during locomotion, we computed the integral of the EMG envelopes of each muscle along different portions of the gait cycle: from foot-strike to mid-stance (i.e., mid-point between foot-strike and foot-off), from mid-stance to foot-off, from foot-off to mid-swing (i.e., mid-point between foot-off and the next foot-strike), and from mid-swing to the next foot-strike. For each of these portions of the gait cycle, we averaged the integrated EMGs across strides, for each animal and experimental condition. We then compared these stride-averaged measures before and after lidocaine and sham injections.

We also evaluated the influence of joint afferents on limb kinematics. We calculated the range of motion (i.e., maximum minus minimum angle across the gait cycle) of hip, knee, and ankle joint, as well as the values of these joint angles at foot-strike, mid-stance, foot-off, and mid-swing. These values were averaged across strides, for each animal and each experimental condition. We also calculated general spatiotemporal gait parameters such as the percentage of stance (duration of the stance phase in percentage of the entire stride) and the step duration (time difference between two consecutive foot-strikes) before and after the injections.

Statistics

We used linear mixed effect models (LMEM) to analyze both EMG and kinematic data using the nlme package in the R environment. LMEMs allowed us to cope with missing data, and to take into account variability at different levels of the data set (e.g., across animals, pre/postinjection, and across injection types). After fitting the LMEMs, we performed the analysis of variance (ANOVA) on the fitted models. If there were statistically significant differences in these general tests, we performed multiple post hoc comparisons to evaluate statistical differences between pre- and postinjections (both for lidocaine and sham) on the dependent variable under investigation, using two-tail *z*-tests and adjusting the *P* values using Bonferroni corrections.

Before fitting the LMEMs to the correlation coefficients between the integrated EMGs, we transformed the data with the Fisher z-transform. This transformation renders the sample distribution of Pearson correlation coefficients approximately normal (31). We confirmed this assumption, as well as the assumptions of independence of residuals and random effects (32) by visually inspecting the distributions using qq-plots and histograms. We then fit a LMEM to the Fisher-transformed correlation coefficients for each pair of muscles, using Time relative to injection (pre/post), Injection type (lidocaine/sham), and their interaction as independent variables. We also considered animal-id as a random effect on the model intercept, effectively implementing a repeated-measures analysis.

To evaluate whether the obtained differences in the correlation coefficients were driven by differences in the covariance or by differences in the individual variances of the integrated EMGs, we fit an LMEM to the numerator (covariance) and an LMEM to the denominator (product of individual standard deviations) of the population Pearson correlation coefficients for each muscle pair. Before fitting these models, the covariances and variances were initially log-transformed to render the distributions approximately normal. We fit these models to the data that showed significant differences before and after lidocaine injection (but not sham) and, therefore, used only a fixed effect of time relative to lidocaine injection with a random-effect of animal-id.

Similarly to the analysis on the integrated EMGs, we fitted a LMEM to the Fisher-transformed stride-averaged correlation coefficients between the EMG time-varying envelopes of each pair of quadriceps muscles. We used Time relative to injection (pre/post), Injection type (lidocaine/sham), and their interaction as fixed effects (independent variables), and animal-id as a random effect.

To evaluate the effect of the injections on individual muscle activity, we fit an LMEM to the log-transformed stride-averaged integral of the EMGs of each individual muscle for each portion of the gait cycle. Similarly, we fit a LMEM to the range of motions (ROM) of each joint, a LMEM to each spatiotemporal gait parameter, and a LMEM to the stride-averaged values of each joint angle at foot-strike, mid-stance, foot-off and mid-stance. For all these models, we used Time relative to injection (pre/post), Injection type (lidocaine/sham), and their interaction as fixed effects (independent variables), and animal-id as a random effect.

RESULTS

Reduction of VM-VI and VL-VI, but Not of VL-VM Across-Stride Correlations, after Inhibition of Knee Sensory Afferents

The scatter plots in Fig. 2 illustrate the covariations between the integrated EMGs of the vasti muscles across

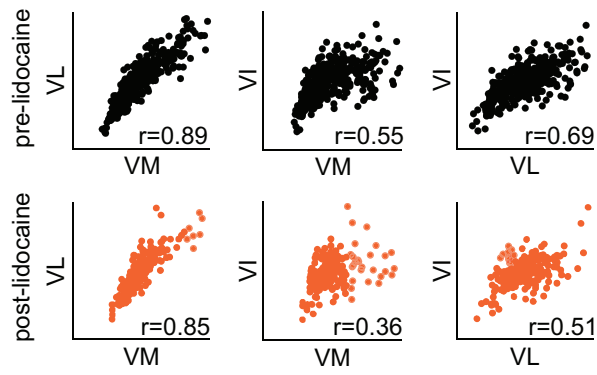

Figure 2. Across-stride correlations between the integrals of the electromyographic (EMG) envelopes before and after lidocaine injection for a representative animal. The (*x*–*y*) coordinates of each dot represent the integrals of the EMG envelopes of a pair of vasti muscles along the stance phase of one stride of locomotion. Hence, there are as many dots as the number of strides, and the correlation coefficient between these measures indicates the strength of correlation between muscle activity across strides. The correlation coefficients are indicated at the bottom of the plots, showing a preferential reduction of vastus medialis (VM)-vastus intermedius (VI) and vastus lateralis (VL)-vastus intermedius (VI) correlations after lidocaine injection. Number of strides n_s = 385 ± 10 and 210 ± 6 [means ± standard deviation (SD) across muscle pairs] for pre- and postlidocaine, respectively.

strides for a representative animal, before and after the injection of lidocaine into the knee capsule. Each individual data point indicates the values of the integrated EMGs of a pair of muscles on one stride. In this rat, the correlation coefficient between the integrated EMGs of VM and VL did not change substantially after the injection of lidocaine, but there was a reduction in VM-VI ($\Delta r = -0.19$) and VL-VI ($\Delta r = -0.18$) correlation coefficients.

Similar results were obtained across animals (Fig. 3). Analysis of variance (Table 1) showed no significant difference between the pre-lidocaine and the post-lidocaine correlation coefficients between VM and VL (no significant effect of the factor Time, i.e., pre-post injection) for both lidocaine and sham (no significant interaction between Time and Injection type). However, there was a significant effect of Time and a significant interaction with Injection type for VM-VI and VL-VI correlations. Post hoc tests revealed a significant reduction in the strength of correlation between the integrated EMGs of these muscle pairs after lidocaine but not after sham injection (Table 2). Similar to VM-VL correlations, we found no significant differences between the correlation coefficients pre- and postinjection for the muscle pairs RF-VM, RF-VL, and RF-VI for either injection type (ANOVA, Table 1) for both lidocaine and sham.

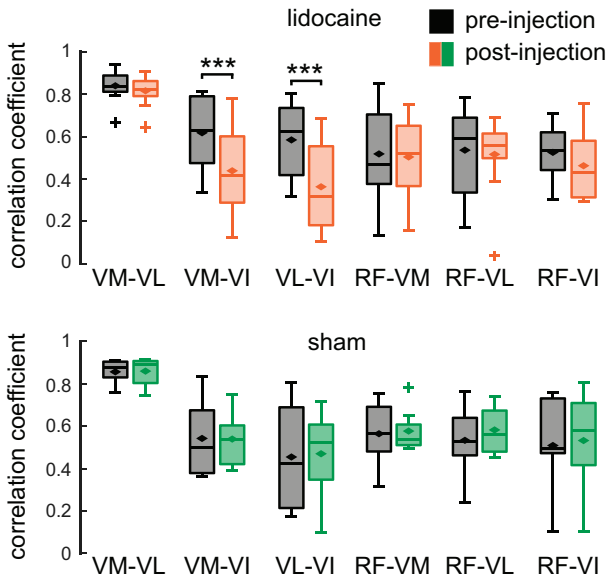

Figure 3. Across-stride correlations among the integrals of the electromyographic (EMG) envelopes of the quadriceps muscles before and after lidocaine and sham injections. The box-whisker plots report the correlation coefficients between the integrated EMG envelopes of each pair of quadriceps muscles before (black) and after the injection of lidocaine (orange, *top*) and sham (green, *bottom*) for all animals (boxes: first quartile, median, and third quartile; whiskers: 1.5 interquartile ranges above and below the first and the fourth quartile; diamonds: means across animals). Notice the reduction of vastus lateralis (VL)-vastus intermedius (VI) and vastus medialis (VM)-VI correlation coefficients after lidocaine but not after sham injection. $n_{lidocaine}$ = 12, 8, 8, 12, 12, 8 and n_{sham} = 9, 6, 6, 9, 9, 6 animals contributed to VM-VL, VM-VI, VL-VI, rectus femoris (RF)-VM, RF-VL, RF-VI correlations, with an average number of strides n_s = 169 ± 94 and 166 ± 56 for lidocaine and sham, respectively. Due to the inclusion criteria (see METHODS) not all animals contributed to each bar. Significance levels: ***$P < 0.001$.

Table 1. *ANOVA of the correlation coefficients between the integrals of the EMG envelopes of each pair of quadriceps muscles*

	VM-VL	VM-VI	VL-VI	RF-VM	RF-VL	RF-VI
Time	0.54	**0.02**	**0.01**	0.79	0.86	0.81
Injection	0.09	0.99	0.85	0.22	0.45	0.57
Time:Injection	0.33	0.05	**0.01**	0.72	0.28	0.44

P values (significant in bold) associated to the factors Time (pre/postinjection), Injection (lidocaine/sham), and their interaction, for each pair of quadriceps muscles. Number of animals $n_{lidocaine}$ = 12, 8, 8, 12, 12, 8 and n_{sham} = 9, 6, 6, 9, 9, 6 for vastus medialis (VM)-vastus lateralis (VL), VM-vastus intermedius (VI), VL-VI, rectus femoris (RF)-VM, RF-VL, RF-VI, respectively. Number of strides n_s = 169 ± 94 and 166 ± 56 (means ± SD) for lidocaine and sham, respectively.

Reduction of Across-Strides Correlations Is Driven by Decreased Covariations among the Vasti Muscles

We evaluated whether the reduction in the correlation coefficients between VM and VI, and between VL and VI obtained after the injection of lidocaine was driven by a reduction in the across-stride covariation of the integrated EMGs of the two muscles (i.e., numerator of the Pearson correlation coefficient; see METHODS), or by an increase in the across-stride variability of each individual muscle's integrated EMGs (denominator of the Pearson correlation coefficient). Figure 4 illustrates the postinjection values of variability (standard deviations) and covariances of the integrated EMGs for each pair of vasti muscles, normalized to their preinjection values. The injection of lidocaine did not cause any consistent effect on the product of the standard deviations for any muscle pair, with some animals showing an increase and others a decrease of this measure following the injection. Accordingly, we found no significant differences between the products of the standard deviations of the integrated EMGs obtained pre- and those obtained postlidocaine injection (ANOVA, VM-VL: P_{time} = 0.4284; VM-VI: P_{time} = 0.7318; VL-VI: P_{time} = 0.9682). Neither was there a significant difference between the pre- and postinjection values of the covariances between the integrated EMGs of VM and VL (ANOVA, P_{time} = 0.2890), hence resulting in no change in the correlation coefficient following lidocaine

Table 2. *Post hoc tests to compare the correlation coefficients between the integrated EMG envelopes across time-to-injection*

	VM-VI		VL-VI	
	Lidocaine	Sham	Lidocaine	Sham
P value	**<0.001**	1	**<0.001**	1
Effect sz.	−0.26	−0.03	−0.31	−0.01
CI	(−0.41; −0.11)	(−0.21; 0.14)	(−0.45; −0.16)	(−0.18; 0.16)

Bonferroni-corrected *P* values (significant in bold), effect sizes (effect sz.), and confidence intervals (CI) of the post hoc tests comparing the difference between post- and preinjection correlation coefficients (i.e., post minus pre injection Fisher-transformed correlation coefficients). The post hoc tests were performed only for those muscle pairs whose correlation coefficients were significantly affected by the factor Time (see ANOVA in Table 1). EMG, electromyography; VI, vastus intermedius; VL, vastus lateralis; VM, vastus medialis.

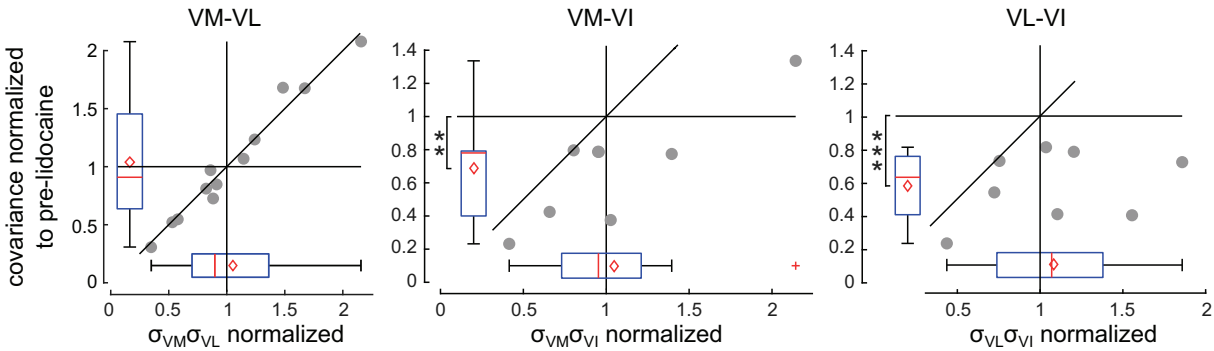

Figure 4. Changes of covariances and individual variances of the integrated electromyographic (EMG) envelopes of the vasti muscle after the injection of lidocaine. Dots represent the covariances (numerator of the population Pearson correlation coefficient) and the product of the individual standard deviations (denominator) after the injection of lidocaine of each animal, normalized to preinjection. These data are summarized in the box-whisker plots (boxes: first quartile, median, and third quartile; whiskers: 1.5 interquartile ranges above and below the first and the fourth quartile; diamonds: means). The data-points below the diagonal ($x = y$) indicate a reduction of the correlation coefficients after lidocaine injection [see vastus medialis (VM)-vastus intermedius (VI) and vastus lateralis (VL)-VI], that could be obtained either by a reduction of the covariance (i.e., data below the horizontal $y = 1$ line) or by an increase of the product of the individual variances (i.e., data to the right of the vertical $x = 1$ line). Although the observed changes in the individual variances after the injection of lidocaine are inconsistent across animals, there is a very consistent reduction of the covariance between the integrated EMG envelopes for VM-VI and VL-VI. Notice that these normalization have been applied only for graphical purpose but not for the analyses, where the data before and after lidocaine injection were directly compared (see METHODS). n and n_s as indicated in Fig. 3. $^{**}P < 0.01$, $^{***}P < 0.001$.

injection for this muscle pair as discussed earlier (Fig. 3). On the other hand, there was a consistent reduction of the covariances between the integrated EMGs of VM and VI, and between those of VL and VI after the injection of lidocaine for all but one animal, leading to a significant difference between their pre- and postinjection values (VM-VI: $P = 0.007$; VL-VI: $P < 0.001$).

No Effect of Knee Joint Sensory Afferents Inhibition on the Correlations among the Activation Time Profiles of the Quadriceps Muscles within the Gait Cycle

We then evaluated the effects of knee joint sensory afferents inhibition on the correlations between the time-varying profile of quadriceps muscles activity within the gait cycle of each individual stride (Fig. 5). This measure of correlation characterizes the fine time scale, moment-to-moment, covariation between muscles within each stride, in contrast to the correlation between the integrated activity of muscles across strides described in the previous sections. We found no differences in the correlation coefficients between the EMG envelopes of any pairs of quadriceps muscles for both lidocaine and sham (ANOVA, Table 3). Although the interaction term between Time and Injection is close to significance for VM-VL ($P = 0.06$), post hoc tests confirm that the strength of correlation between the EMG envelopes of these two muscles is not significantly affected by the injection of either lidocaine ($P = 0.56$) or sham ($P = 0.17$).

No Effect of Knee Sensory Afferents Inhibition on the Activity of Individual Quadriceps Muscles

We next evaluated whether inhibition of knee joint sensory afferents influenced the activity of individual muscles within the gait cycle. Figure 6 (*top*) illustrates that the time course of the EMG envelopes of the quadriceps muscles are minimally affected by the injection of lidocaine into the knee capsule. Postlidocaine, the activity of the vasti muscles seems to be slightly higher than prelidocaine after mid-stance (VM and VL) or at the beginning of the stance phase (VI). However, these differences are not statistically significant, likely due to variability across animals (Fig. 6, *bottom*). Indeed, the pre- and postinjection integrated EMGs are not significantly different for any muscle, any portion of

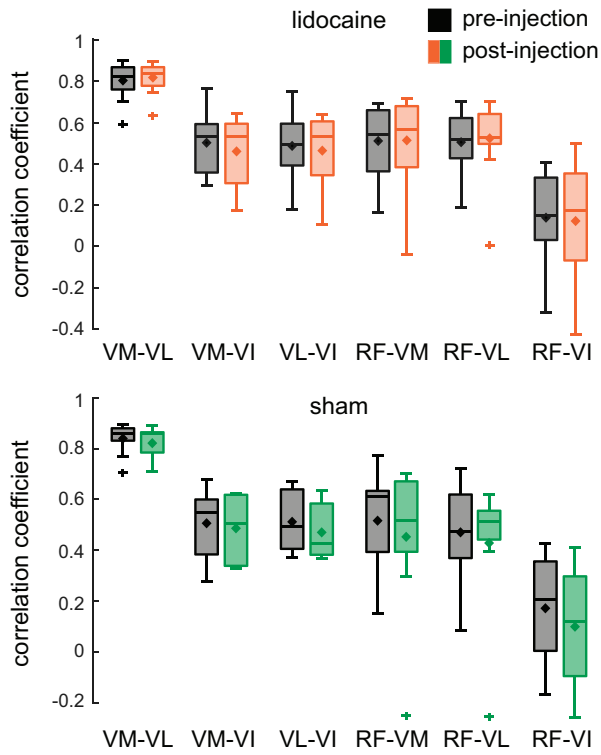

Figure 5. Correlations among the time-profiles of the electromyographic (EMG) envelopes of the quadriceps muscles before and after lidocaine and sham injections. The box-whisker plots report the stride-averaged correlation coefficients between the time-profiles of the EMG envelopes of each pair of quadriceps muscles before (black) and after the injection of lidocaine (orange, *top*) and sham (green, *bottom*) for all animals. $n_{lidocaine}$ = 12, 8, 8, 12, 12, 8 and n_{sham} = 9, 6, 6, 9, 9, 6 animals contributed to vastus medialis (VM)-vastus lateralis (VL), VM-vastus intermedius (VI), VL-VI, rectus femoris (RF)-VM, RF-VL, RF-VI correlations, with an average number of strides $n_s = 169 \pm 94$ and 163 ± 51 for lidocaine and sham, respectively.

Table 3. *ANOVA of the correlation coefficients between the time-profiles of the EMG envelopes of each pair of quadriceps muscles*

	VM-VL	VM-VI	VL-VI	RF-VM	RF-VL	RF-VI
Time	0.57	0.37	0.34	0.31	0.68	0.19
Injection	0.91	0.80	0.83	0.22	0.04	0.99
Time:Injection	0.06	0.78	0.79	0.15	0.17	0.36

P values associated to the factors *Time* (pre/postinjection), *Injection* (lidocaine/sham) and their interaction, for each pair of quadriceps muscles. n and n_s as in Fig. 5. EMG, electromyography; VI, vastus intermedius; VL, vastus lateralis; VM, vastus intermedius; RF, rectus femoris.

the gait cycle, and independently on the injection type (ANOVA results presented in Table 4). Notice we did not perform these analyses at swing-init for VM, VL, and VI, as the vasti muscles are inactive in this portion of the gait cycle (Fig. 6).

No Effect of Knee Sensory Afferents Inhibition on Movement Kinematics

Consistent with the lack of change in individual muscle activity after lidocaine injection, inhibition of knee sensory afferents caused no significant alterations in movement kinematics. Figure 7 illustrates the average limb-stick figures (see Fig. 1 for anatomical interpretation) at different moments of the gait cycle, and suggests minimal differences between pre- and postinjection kinematics for both lidocaine (Fig. 7*A*) and sham injections (Fig. 7*B*). Accordingly, the spatiotemporal gait parameters (Fig. 7, boxplots) were not affected by any of the injections, with no significant differences between pre- and postinjection for percentage of stance (ANOVA: P_{time} = 0.9503, $P_{time:inj}$ = 0.3304) and step duration (ANOVA: P_{time} = 0.6975, $P_{time:inj}$ = 0.9815).

The analysis of individual joint angles further confirms these results, suggesting that the inhibition of knee sensory afferents does not affect limb kinematics (Fig. 8, ANOVA results reported in Table 5). Indeed, we observed small changes in limb kinematics following both lidocaine and sham injections. The pre- and postinjection values of the hip angle were significantly different to one another at foot-strike for both lidocaine and sham injections, and nonsignificantly different at mid-stance, foot-off, and mid-swing. The knee angles pre- and postinjection of lidocaine as well as sham were significantly different to one another at foot-strike, mid-stance, and foot-off, but not at mid-swing. Finally, the preinjection values of the ankle angle were not significantly different from the postinjection values at any point of the gait cycle for both lidocaine and sham. Finally, we found no significant differences between the pre- and postinjection joint range of motions (ROM, Fig. 8 boxplots) for the hip (ANOVA: P_{time} = 0.6949, $P_{time:inj}$ = 0.6087), knee (ANOVA: P_{time} = 0.6031, $P_{time:inj}$ = 0.0871), and ankle (ANOVA: P_{time} = 0.3188, $P_{time:inj}$ = 0.4137).

DISCUSSION

We examined whether joint sensory afferents originating from the knee modulated the correlations between quadriceps muscles activity during locomotion in the rat. Injection of lidocaine into the knee capsule was used to silence knee joint sensory afferents. There was no significant change in the correlations between the time-varying profiles of muscle activity within the gait cycle for any quadriceps muscle pair. Similarly, there was no significant change in the across-stride correlations between the integrated EMGs of VL and VM, nor between the integrated EMGs of RF and any of the vasti muscles. On the other hand, the inhibition of knee joint

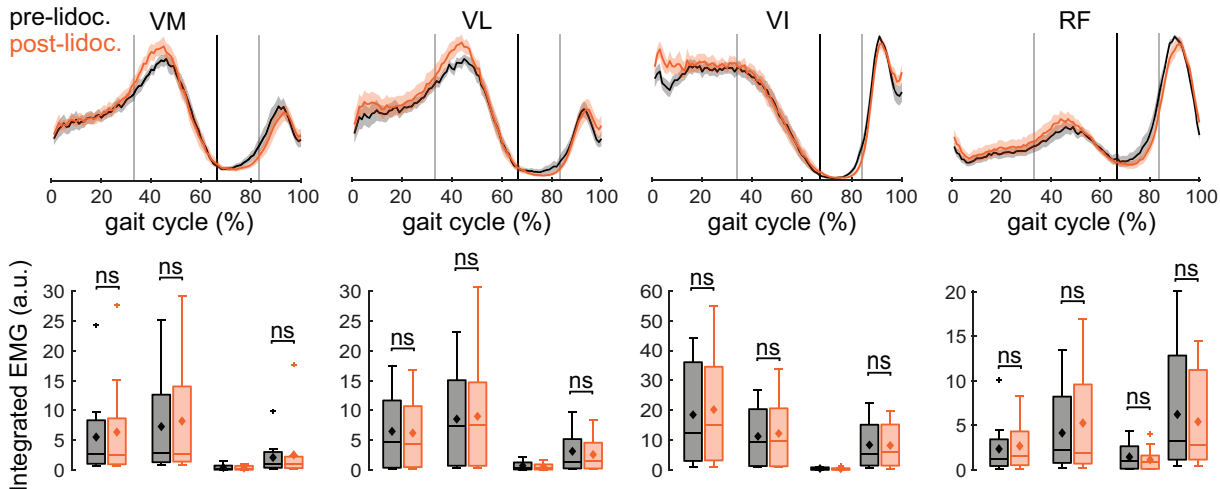

Figure 6. Activity of individual quadriceps muscles before and after the injection of lidocaine. *Top*: electromyographic (EMG) envelopes of the quadriceps muscles across the gait cycle before (black) and after (orange) the injection of lidocaine. Data are averaged across strides and then across animals; the shaded areas indicate standard errors across animals. The gait cycle starts at the moment of foot-strike. The black vertical lines indicate the moment of foot-off, and the gray vertical lines indicate mid-stance and mid-swing (all averaged across strides, animals, and conditions—the moment of foot-off was unaffected by the injection of lidocaine as indicated in Fig. 7). *Bottom*: integrals of the EMG envelopes within each portion of the gait cycle (boxes: first quartile, median, and third quartile; whiskers: 1.5 interquartile ranges above and below the first and the fourth quartile; diamonds: mean across animals). $n_{lidocaine}$ = 12, 12, 9, 8 and n_{sham} = 9, 9, 7, 9 for vastus medialis (VM), vastus lateralis (VL), vastus intermedius (VI), and rectus femoris (RF), respectively; n_s = 173 ± 96 and 170 ± 57 for lidocaine and sham, respectively. The vasti muscles are silent between foot-off and mid-swing, and therefore this portion of the gait cycle was not analyzed for these muscles.

Table 4. *ANOVA of the individual quadriceps activity*

	VM				VL				VI				RF			
	Stance		Swing		Stance		Swing		Stance		Swing		Stance		Swing	
	Init	End	Init	End	Init	End	Init	End	Init	End	Init	End	Init	End	Init	End
Time	0.62	0.66	0.59		0.28	0.46	0.36		0.32	0.99	0.87		0.55	0.88	0.40	0.23
Injection	0.49	0.09	0.42		0.24	0.89	0.14		0.82	0.81	0.54		0.13	0.05	0.17	0.01
Time:Injection	0.89	0.78	0.12		0.95	0.81	0.18		0.74	0.58	0.54		0.57	0.40	0.07	0.90

P values associated with the factors Time, Injection, and their interaction term, for each muscle and portion of the gait cycle. Number of animals $n_{lidocaine}$ = 12, 12, 9, 8 and n_{sham} = 9, 9, 7, 9 for vastus intermedius (VM), vastus lateralis (VL), vastus intermedius (VI), and rectus femoris (RF), respectively; number of strides n_s = 173 ± 96 and 170 ± 57 (means ± SD) for lidocaine and sham, respectively. The vasti muscles are silent between foot-off and mid-swing, and therefore this portion of the gait cycle was not analyzed for these muscles.

sensory afferents caused a significant reduction in the across-stride correlations between the integrated EMGs of VM and VI, and between those of VL and VI. This reduced correlation strength originated from a lower across-stride covariation between the integrated EMGs of these muscles, and not from an increased variability of the integrated EMGs of the individual muscles. Taken together, these results suggest that knee joint sensory afferents contribute to the coordinated activity between VI and the other vasti muscles across strides.

We previously showed that the activity of VM and VL are strongly correlated during locomotion. The integrals of their EMG envelopes were highly correlated across strides, and the time profiles of these envelopes were highly correlated within the gait cycle of each individual stride (21). Since VM and VL have opposite actions on the mediolateral forces on the patella (22), such strong correlations are consistent with a strategy that limits the mediolateral loading on the patellofemoral joint (12, 13, 24, 33): variations in the lateral force applied by VL on the patella are compensated by similar variations in the medial force applied by VM. The fact these muscles' activity is correlated both across strides and within each individual stride suggests that patellar loads are minimized both at a coarse time resolution, from one stride to the next, and at a fine time resolution, from moment-to-moment within each stride. Here, we hypothesized that these correlations depended on knee joint sensory afferents. Indeed, sensory receptors within the knee (9) provide the CNS with critical information about strains in ligaments, stresses between bones and within cartilaginous structures, as well as about deformations of the joint capsule, which could all be involved in feedback circuitries that aim at limiting joint loading (34) and maintaining dynamic joint stability (11). If the strong correlations between the activity of VM and VL originate from such feedback loops, inhibiting knee joint sensory afferents should cause a reduction in the strength of these correlations.

However, we found no change in the strength of VM-VL correlation either across-strides or within the gait cycle following the inhibition of knee joint sensory afferents, suggesting that the regulation of stresses and strains in the patellofemoral joint is implemented by different neural mechanisms. For example, spinal reflexes mediated by muscle spindles (35) or Golgi tendon organs (36) may compensate for excessive differences between the length or tension of VM and VL, resulting in the coordinated activity of these two

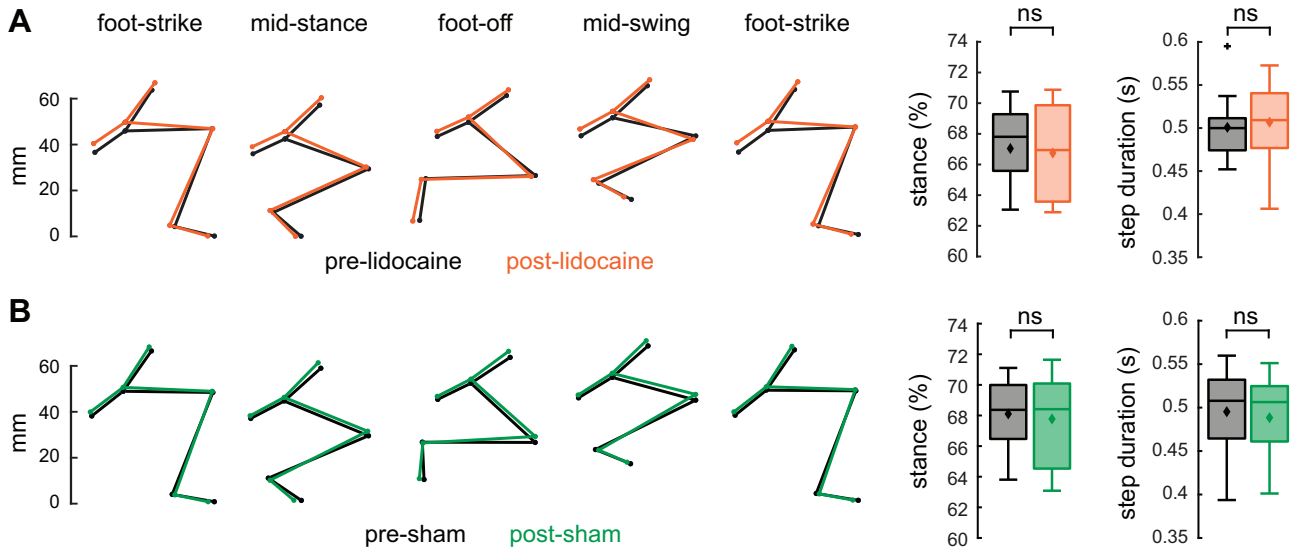

Figure 7. Gait parameters before and after lidocaine and sham injection. The average limb-stick figures suggest minimal differences in the pose of the animals before (black) and after lidocaine (*A*; orange) and sham (*B*; green) injections at different points of the gait cycle (foot-strike, mid-stance, foot-off, mid-swing, foot-strike). The box-whisker plots to the right illustrate the percentage of stance and the step duration (boxes: first quartile, median, and third quartile; whiskers: 1.5 interquartile ranges above and below the first and the fourth quartile; diamonds: mean across animals), showing no significant differences before and after the injections. $n_{lidocaine}$ = 12, n_{sham} = 9; n_s = 238 ± 114 and 236 ± 71 for lidocaine and sham, respectively.

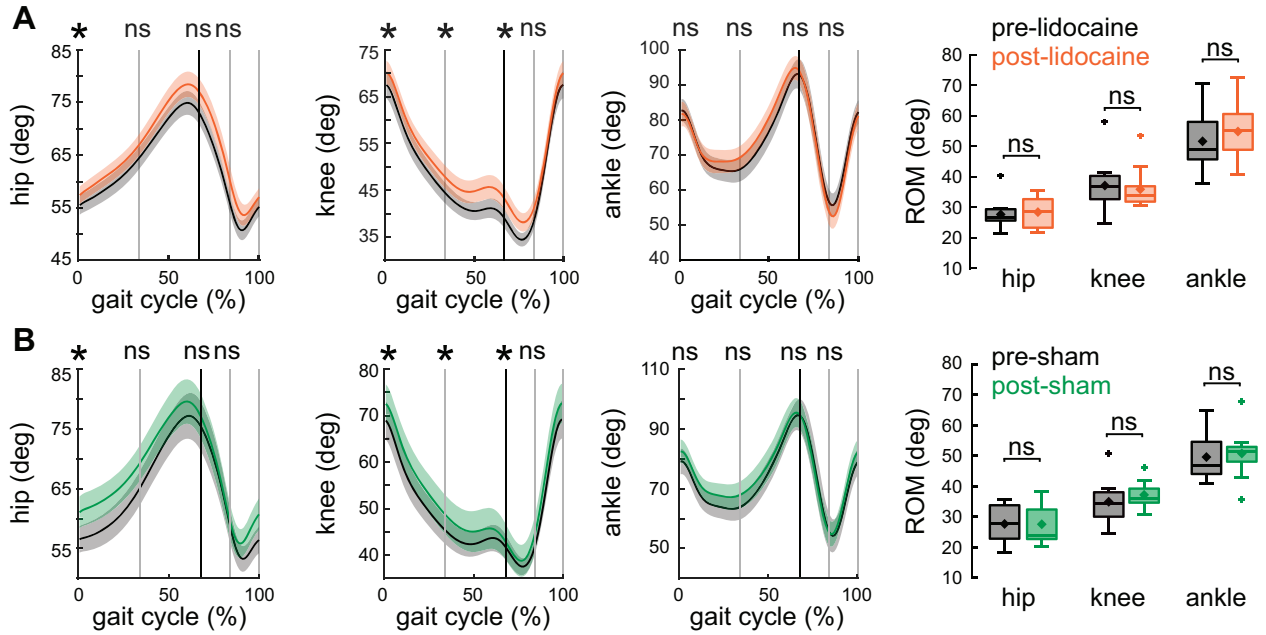

Figure 8. Effect of inhibition of knee sensory afferents on joint angles. The plots on the left illustrate the joint angles across the gait cycle before (black) and after lidocaine (*A*; orange) and sham (*B*; green) injections. Data are averaged across strides and then across animals (means ± SE). The gait cycle starts at the moment of foot-strike. The vertical black lines represent the average moment of foot-off; the vertical gray lines represent the average mid-stance, mid swing, and the average moment of foot-strike. The box-whisker plots on the right indicate no difference in the range of motion (ROM) of any joint before and after lidocaine and sham injection (boxes: first quartile, median, and third quartile; whiskers: 1.5 interquartile ranges above and below the first and the fourth quartile; diamonds: mean). *n* and n_s like in Fig. 7. *$P < 0.05$.

muscles. Alternatively, last order spinal interneurons might project to the motoneurons of both VM and VL. This hypothetical common premotor drive to VM and VL was indeed previously measured (25) and could originate from both spinal or cortical systems (37). Additional work is necessary to dissect the neural circuitry underlying the regulation of patellofemoral joint loading, particularly relevant to uncover the potential neural bases of patellofemoral pain (24).

Although knee joint sensory afferents did not appear to drive correlations between VM and VL, our results suggested that these afferents contribute to the across-stride correlation between the integrated EMG envelopes of VI and those of the other vasti muscles. The reduced correlation strength between the integrated EMG envelopes of VI and those of both VM and VL after the injection of lidocaine suggests the existence of feedback loops mediated by knee joint sensory afferents that coordinate the activations of these pairs of muscles. Joint sensory afferents may lead to common presynaptic drives to VI-VM and to VI-VL, coupling the activity of these muscle pairs and potentially resulting in previously described muscle synergies (38–41) mediated by sensory feedback (42). These circuitry are likely polysynaptic (26) and may involve either the α or the γ systems (11). Interestingly, VI and VL are coupled through long latency force feedback in the cat, whereas VM and VL are not (the connection between VM and VI was not determined; 43); although the contribution of this inhibitory feedback to the correlations described here is unclear, those results are consistent with the specificity of sensory feedback pathways among vasti muscles suggested by the present study. Furthermore, our results are consistent with previous studies demonstrating that feedback circuitry in the spinal cord respond to stresses and strains in joint structures such as the anterior cruciate ligament (34, 44) and the meniscus (45).

The functional role of these correlations between VI and the other vasti muscles is not obvious. One possibility is that, like the correlations between VM and VL, they contribute to stabilization of knee joint structures, including the patellofemoral joint. Although VI has a limited influence on the mediolateral loading on the patella [its line of force has minimal components on that axis (46)], the across-stride correlation between VI and the other vasti muscles could help lock the patella in the femoral groove or increase patellofemoral contact forces to prevent patellar displacement during strong

Table 5. *ANOVA of joint angles*

	Hip				Knee				Ankle			
	Foot-Strike	Mid-Stance	Foot-off	Mid-Swing	Foot-Strike	Mid-Stance	Foot-off	Mid-Swing	Foot-Strike	Mid-Stance	Foot-off	Mid-Swing
Time	**0.03**	0.07	0.15	0.13	**0.02**	**0.02**	**0.04**	0.07	0.70	0.16	0.60	0.97
Injection	0.26	0.59	0.74	0.86	0.88	0.82	0.92	0.17	0.41	0.65	0.27	0.90
Time:Injection	0.36	0.67	0.70	0.46	0.71	0.95	0.45	0.95	0.36	0.99	0.87	0.40

P values (significant in bold) associated to the factors Time, Injection, and their interaction term, for each joint and moment of the gait cycle. Number of animals $n_{lidocaine}$ = 12 and n_{sham} = 9; number of strides n_s = 238 ± 114 and 236 ± 71 (means ± SD) for lidocaine and sham, respectively.

quadriceps contractions. Alternatively, the covariation of all the vasti muscles could reflect a more general strategy to share muscle effort across close synergists (47, 48) during the generation of knee extension torque. Although additional biomechanical analyses and perturbations will be necessary to test these ideas, our results suggest that knee joint afferents are at least partially responsible for these correlations between VI and the other vasti muscles.

We examined correlations between quadriceps muscles at two different levels of temporal resolution: across-stride correlations among integrated EMGs over the stance phase of locomotion, and correlations among the time profile of the EMG envelopes within the gait cycle. The former measure provides information about muscle coordination at a coarse time scale, evaluating covariations across repetitions of the same movement (i.e., repeated strides). Similar across-repetition correlations of motor-related variables (e.g., muscle activity or movement kinematics) are used as measures of motor coordination in current motor control theories (49), including to evaluate the risk of knee osteoarthritis (50). However, previous studies have suggested that correlations between muscle activity are also expressed at a much finer time scale, for example in the firing rates of vasti motor units (25). We found here that lidocaine only affected correlations at coarse time scales; the fine time scale correlations between time-varying EMG profiles were unaltered by lidocaine. These results might reflect the slow temporal dynamics of joint sensory afferents in response to changes in joint loads (26), so that joint afferents only signal changes in joint load at the course time scales necessary to drive across-stride correlations. Finer time scale correlations might be driven either by other sensory afferents with faster dynamics, such as muscle proprioceptors, or by feedforward pathways in spinal or supraspinal systems. Future experiments evaluating the effect of lidocaine on the coherence between motor unit firing rates, or evaluating the effect of manipulating the activity of other sensory afferents might help further elucidate these possibilities.

Neither the activity of any individual muscle within the gait cycle (Fig. 6) nor the across-stride variability of this activity (Fig. 4) was affected by the injection of lidocaine, suggesting that joint sensory afferents have minimal influence on the activity of individual quadriceps muscles. This result is consistent with previous studies on humans, in which injection of intra-articular local anesthetic (lidocaine or bupivicaine) into the knee or the ankle joints did not alter muscle activation patterns (18, 19). Similarly, we observed no specific effect of lidocaine on limb kinematics during locomotion; although there were small changes in limb kinematics after lidocaine injections, these changes were similar to those observed after sham injections (Fig. 8), suggesting that they were likely due to nonspecific factors such as fatigue over the time course of the experiment. Thus, we found no evidence that knee joint afferents played a substantial role in task performance (15).

It is important to note that we examined the potential role of knee joint sensory afferents in a single behavioral condition (treadmill locomotion on a level surface) and only after temporary inhibition (transient inhibition lasting ~1 h). It is possible that knee afferents would play a more significant role in other task conditions in which joint stresses or strains might be especially large (e.g., jumping or landing). Similarly, joint sensory afferents might play a more important role in long-term alterations in muscle activations; e.g., they might signal persistent alterations in joint stresses caused by injuries or normal aging, driving adaptations in muscle activity over days. Consistent with this possibility, the chronic inhibition of joint sensory afferents has been shown to contribute to the development of joint diseases such as osteoarthritis (16, 17). We also note that, although there are many similarities between the knee joint of rats and humans, in rats the patella sits within a very deep intercondylar groove across the entire range of motion whereas in humans the patella is stabilized only by the lateral facet of the groove and primarily during knee flexion. Performing the present study on rats allowed us to more easily record the activity of VI during dynamic movements, showing that joint sensory afferents may be involved in muscle coordination. Nonetheless, additional experiments should be performed to evaluate these results on humans.

Our results also suggest that damage to internal joint structures containing sensory receptors (i.e., ligaments, joint capsule) should be considered sensorimotor, and not only biomechanical injuries. Injuries compromising knee joint receptors [e.g., anterior cruciate ligament (ACL) rupture (51)] might affect the coordination between the vasti muscles. To the extent that such coordination is involved in regulating joint stresses or strains, the loss of this sensory feedback might contribute to the development of long-term conditions like osteoarthrosis (16, 52). Recent studies have also shown that these injuries alter the activity of higher neural areas (53). Whether these changes reflect the lost sensory feedback from the knee joint, adaptive neural control strategies to compensate for the altered joint mechanics (12, 13), or maladaptive changes (54, 55) due to joint pain or other factors remains unclear. In any case, these observations suggest that rehabilitation strategies following joint injuries should not only consider the mechanical consequences of the injury, but their potential effect on sensory processing and neural control.

DATA AVAILABILITY

Data will be made available upon reasonable request.

GRANTS

This research was supported by the National Institutes of Health (NIH) Grant Number NS086973 (to M. C. Tresch) and National Science Foundation Grant DBI-2015317 (to M. C. Tresch).

DISCLOSURES

No conflicts of interest, financial or otherwise, are declared by the authors.

AUTHOR CONTRIBUTIONS

C.A. and M.C.T. conceived and designed research; C.A., A.P., and D.P.T. performed experiments; C.A. analyzed data; C.A. and M.C.T. interpreted results of experiments; C.A. prepared figures; C.A. and M.C.T. drafted manuscript; C.A., A.P., D.P.T., and M.C.T. edited and revised manuscript; C.A., A.P., D.P.T., and M.C.T. approved final version of manuscript.

REFERENCES

1. **Proske U**, **Gandevia S.** The proprioceptive senses: their roles in signaling body shape, body position and movement, and muscle force. *Physiol Rev* 92: 1651–1697, 2012. doi:10.1152/physrev.00048.2011.
2. **Goodman JM**, **Tabot GA**, **Lee AS**, **Suresh AK**, **Rajan AT**, **Hatsopoulos NG**, **Bensmaia S.** Postural representations of the hand in the primate sensorimotor cortex. *Neuron* 104: 1000–1009.e7, 2019. doi:10.1016/j.neuron.2019.09.004.
3. **Li L**, **Zhang S**, **Dobson J.** The contribution of small and large sensory afferents to postural control in patients with peripheral neuropathy. *J Sport Heal Sci* 8: 218–227, 2019. doi:10.1016/j.jshs.2018.09.010.
4. **Relph N**, **Herrington L**, **Tyson S.** The effects of ACL injury on knee proprioception: a meta-analysis. *Physiotherapy* 100: 187–195, 2014. doi:10.1016/j.physio.2013.11.002.
5. **Akay T**, **Tourtellotte WG**, **Arber S**, **Jessell TM.** Degradation of mouse locomotor pattern in the absence of proprioceptive sensory feedback. *Proc Natl Acad Sci USA* 111: 16877–16882, 2014. doi:10.1073/pnas.1419045111.
6. **Gordon J**, **Ghilardi MF**, **Ghez C.** Impairments of reaching movements in patients without proprioception. I. Spatial errors. *J Neurophysiol* 73: 347–360, 1995. doi:10.1152/jn.1995.73.1.347.
7. **Bornstein B**, **Konstantin N**, **Alessandro C**, **Tresch MC**, **Zelzer E.** More than movement: the proprioceptive system as a new regulator of musculoskeletal biology. *Curr Opin Physiol* 20: 77–89, 2021. doi:10.1016/j.cophys.2021.01.004.
8. **Blecher R**, **Krief S**, **Galili T**, **Biton IE**, **Stern T**, **Assaraf E**, **Levanon D**, **Appel E**, **Anekstein Y**, **Agar G**, **Groner Y**, **Zelzer E.** The proprioceptive system masterminds spinal alignment: insight into the mechanism of scoliosis. *Dev Cell* 42: 388–399.e3, 2017. doi:10.1016/j.devcel.2017.07.022.
9. **Çabuk H**, **Kuşku Çabuk F.** Mechanoreceptors of the ligaments and tendons around the knee. *Clin Anat* 29: 789–795, 2016. doi:10.1002/ca.22743.
10. **Grigg P**, **Greenspan BJ**, **Greenspan J.** Response of primate joint afferent neurons to mechanical stimulation of knee joint. *J Neurophysiol* 40: 1–8, 1977. doi:10.1152/jn.1977.40.1.1.
11. **Riemann BL**, **Lephart SM.** The sensorimotor system. II. The role of proprioception in motor control and functional joint stability. *J Athl Train* 37: 80–84, 2002. doi:10.1016/j.jconhyd.2010.08.009.
12. **Alessandro C**, **Rellinger BA**, **Barroso FO**, **Tresch MC.** Adaptation after vastus lateralis denervation in rats demonstrates neural regulation of joint stresses and strains. *eLife* 7: e38215, 2018. doi:10.7554/eLife.38215.
13. **Barroso FO**, **Alessandro C**, **Tresch MC.** Adaptation of muscle activation after patellar loading demonstrates neural control of joint variables. *Sci Rep* 9: 20370, 2019. doi:10.1038/s41598-019-56888-9.
14. **Ryan CG**, **Rowe PJ.** An electromyographical study to investigate the effects of patellar taping on the vastus medialis/vastus lateralis ratio in asymptomatic participants. *Physiother Theory Pract* 22: 309–315, 2006. doi:10.1080/09593980601023739.
15. **Ferrell WR**, **Baxendale RH**, **Carnachan C**, **Hart IK.** The influence of joint afferent discharge on locomotion, proprioception and activity in conscious cats. *Brain Res* 347: 41–48, 1985. doi:10.1016/0006-8993(85)90887-X.
16. **Nagelli CV**, **Cook JL**, **Kuroki K**, **Bozynski C**, **Ma R**, **Hewett TE.** Does anterior cruciate ligament innervation matter for joint function and development of osteoarthritis? *J Knee Surg* 30: 364–371, 2017. doi:10.1055/s-0036-1592145.
17. **Salo PT**, **Hogervorst T**, **Seerattan RA**, **Rucker D**, **Bray RC.** Selective joint denervation promotes knee osteoarthritis in the aging rat. *J Orthop Res* 20: 1256–1264, 2002. doi:10.1016/S0736-0266(02)00045-1.
18. **Stone DA**, **Abt JP**, **House AJ**, **Akins JS**, **Pederson JJ**, **Keenan KA**, **Lephart SM.** Local anaesthetics use does not suppress muscle activity following an ankle injection. *Knee Surg Sports Traumatol Arthrosc* 21: 1269–1278, 2013. doi:10.1007/s00167-012-1984-8.
19. **Oksendahl HL**, **Fleming BC**, **Blanpied PR**, **Ritter M**, **Hulstyn MJ**, **Fadale PD.** Intra-articular anesthesia and knee muscle response. *Clin Biomech (Bristol, Avon)* 22: 529–536, 2007. doi:10.1016/j.clinbiomech.2007.01.008.
20. **Sjölander P**, **Johansson HH**, **Djupsjöbacka M.** Spinal and supraspinal effects of activity in ligament afferents. *J Electromyogr Kinesiol* 12: 167–176, 2002. doi:10.1016/S1050-6411(02)00017-2.
21. **Alessandro C**, **Barroso FO**, **Prashara A**, **Tentler DP**, **Yeh HY**, **Tresch MC.** Coordination amongst quadriceps muscles suggests neural regulation of internal joint stresses, not simplification of task performance. *Proc Natl Acad Sci USA* 117: 8135–8142, 2020. doi:10.1073/pnas.1916578117.
22. **Sandercock TG**, **Wei Q**, **Dhaher YY**, **Pai DK**, **Tresch MC.** Vastus lateralis and vastus medialis produce distinct mediolateral forces on the patella but similar forces on the tibia in the rat. *J Biomech* 81: 45–51, 2018. doi:10.1016/j.jbiomech.2018.09.007.
23. **Wilson NA**, **Sheehan FT.** Dynamic in vivo quadriceps lines-of-action. *J Biomech* 43: 2106–2113, 2010. doi:10.1016/j.jbiomech.2010.04.002.
24. **Pal S**, **Besier TF**, **Draper CE**, **Fredericson M**, **Gold GE**, **Beaupre GS**, **Delp SL.** Patellar tilt correlates with vastus lateralis:vastus medialis activation ratio in maltracking patellofemoral pain patients. *J Orthop Res* 30: 927–933, 2012. doi:10.1002/jor.22008.
25. **Laine CM**, **Martinez-Valdes E**, **Falla D**, **Mayer F**, **Farina D.** Motor neuron pools of synergistic thigh muscles share most of their synaptic input. *J Neurosci* 35: 12207–12216, 2015. doi:10.1523/JNEUROSCI.0240-15.2015.
26. **Johansson H**, **Sjölander P**, **Sojka P.** Actions on gamma-motoneurones elicited by electrical stimulation of joint afferent fibres in the hind limb of the cat. *J Physiol* 375: 137–152, 1986. doi:10.1113/jphysiol.1986.sp016110.
27. **Loeb GE**, **Gans C.** *Electromyography for Experimentalists*. Chicago, IL: The University of Chicago Press, 1986.
28. **Overduin SA**, **d'Avella A**, **Roh J**, **Bizzi E.** Modulation of muscle synergy recruitment in primate grasping. *J Neurosci* 28: 880–892, 2008. doi:10.1523/JNEUROSCI.2869-07.2008.
29. **Bauman JM**, **Chang YH.** High-speed X-ray video demonstrates significant skin movement errors with standard optical kinematics during rat locomotion. *J Neurosci Methods* 186: 18–24, 2010. doi:10.1016/j.jneumeth.2009.10.017.
30. **Carlson-Kuhta P**, **Trank TV**, **Smith JL.** Forms of forward quadrupedal locomotion. II. A comparison of posture, hindlimb kinematics, and motor patterns for upslope and level walking. *J Neurophysiol* 79: 1687–1701, 1998. doi:10.1152/jn.1998.79.4.1687.
31. **Bond CF**, **Richardson K.** Seeing the Fisher Z-transformation. *Psychometrika* 69: 291–303, 2004. doi:10.1007/BF02295945.
32. **Pinheiro JC**, **Bates DM.** *Mixed Effects Models in S and S-Plus* (1st ed). New York, NY: Springer, 2000.
33. **Mellor R**, **Hodges P.** Motor unit synchronization between medial and lateral vasti muscles. *Clin Neurophysiol* 116: 1585–1595, 2005. doi:10.1016/j.clinph.2005.04.004.
34. **Solomonow M.** Sensory-motor control of ligaments and associated neuromuscular disorders. *J Electromyogr Kinesiol* 16: 549–567, 2006. doi:10.1016/j.jelekin.2006.08.004.
35. **Macefield VG**, **Knellwolf TP.** Functional properties of human muscle spindles. *J Neurophysiol* 120: 452–467, 2018. doi:10.1152/jn.00071.2018.
36. **Nichols TR.** Distributed force feedback in the spinal cord and the regulation of limb mechanics. *J Neurophysiol* 119: 1186–1200, 2018. doi:10.1152/jn.00216.2017.
37. **Farina D**, **Negro F.** Common synaptic input to motor neurons, motor unit synchronization, and force control. *Exerc Sport Sci Rev* 43: 23–33, 2015. doi:10.1249/JES.0000000000000032.
38. **Tresch M**, **Jarc A.** The case for and against muscle synergies. *Curr Opin Neurobiol* 19: 601–607, 2009. doi:10.1016/j.conb.2009.09.002.
39. **Alessandro C**, **Carbajal JP**, **d'Avella A.** Synthesis and adaptation of effective motor synergies for the solution of reaching tasks. In: *Lecture Notes in Artificial Intelligence (LNAI)*, edited by Ziemke T, Balkenius C, Hallam J. Berlin, Heidelberg: Springer-Verlag, 2012, p. 33–43.
40. **Alessandro C**, **Nori F.** Identification of synergies by optimization of trajectory tracking tasks. In: *Fourth IEEE RAS/EMBS International Conference on Biomedical Robotics and Biomechatronics*. Rome: IEEE, 2012, p. 924–930.
41. **Alessandro C**, **Carbajal JP**, **d'Avella A.** A computational analysis of motor synergies by dynamic response decomposition. *Front Comput Neurosci* 7: 191, 2013. doi:10.3389/fncom.2013.00191.
42. **Santuz A**, **Akay T**, **Mayer WP**, **Wells TL**, **Schroll A**, **Arampatzis A.** Modular organization of murine locomotor pattern in the presence

and absence of sensory feedback from muscle spindles. *J Physiol* 597: 3147–3165, 2019. doi:10.1113/JP277515.
43. **Wilmink RJH**, **Nichols TR.** Distribution of heterogenic reflexes among the quadriceps and triceps surae muscles of the cat hind limb. *J Neurophysiol* 90: 2310–2324, 2003. doi:10.1152/jn.00833.2002.
44. **Seitz AM**, **Murrmann M**, **Ignatius A**, **Dürselen L**, **Friemert B**, **von Lübken F.** Neuromapping of the capsuloligamentous knee joint structures. *Arthrosc Sports Med Rehabil* 3: e555–e563, 2021. doi:10.1016/j.asmr.2020.12.009.
45. **Akgun U**, **Kocaoglu B**, **Orhan EK**, **Baslo MB**, **Karahan M.** Possible reflex pathway between medial meniscus and semimembranosus muscle: an experimental study in rabbits. *Knee Surg Sports Traumatol Arthrosc* 16: 809–814, 2008. doi:10.1007/s00167-008-0542-x.
46. **Wilson NA**, **Sheehan FT.** Dynamic in vivo 3-dimensional moment arms of the individual quadriceps components. *J Biomech* 42: 1891–1897, 2009. doi:10.1016/j.jbiomech.2009.05.011.
47. **Todorov E**, **Jordan MI.** Optimal feedback control as a theory of motor coordination. *Nat Neurosci* 5: 1226–1235, 2002. doi:10.1038/nn963.
48. **Alessandro C**, **Beckers N**, **Goebel P**, **Resquin F**, **Gonzalez J**, **Osu R.** Motor control and learning theories. In: *Emerging Therapies in Neurorehabilitation II*, edited by Pons J, Raya R, Gonzalez J. Switzerland: Springer International Publishing AG, 2016, p. 225–250.
49. **Latash ML**, **Scholz JP**, **Schoener G.** Motor control strategies revealed in the structure of motor variability. *Exerc Sport Sci Rev* 30: 26–31, 2002. doi:10.1097/00003677-200201000-00006.
50. **Tawy GF**, **Rowe P**, **Biant L.** Gait variability and motor control in patients with knee osteoarthritis as measured by the uncontrolled manifold technique. *Gait Posture* 59: 272–277, 2018. doi:10.1016/j.gaitpost.2017.08.015.
51. **Dhillon MS**, **Bali K**, **Prabhakar S.** Proprioception in anterior cruciate ligament deficient knees and its relevance in anterior cruciate ligament reconstruction. *Indian J Orthop* 45: 294–300, 2011. doi:10.4103/0019-5413.80320.
52. **Back D**, **Smith C**, **Wong F**, **Ajuied A**, **Norris M**, **Davies A**, **Earnshaw P.** Anterior cruciate ligament injury and radiologic progression of knee osteoarthritis. *Am J Sports Med* 42: 2242–2252, 2014. doi:10.1177/0363546513508376.
53. **Grooms DR**, **Page SJ**, **Nichols-Larsen DS**, **Chaudhari AMW**, **White SE**, **Onate JA.** Neuroplasticity associated with anterior cruciate ligament reconstruction. *J Orthop Sport Phys Ther* 47: 180–189, 2017. doi:10.2519/jospt.2017.7003.
54. **Needle AR**, **Lepley AS**, **Grooms DR.** Central nervous system adaptation after ligamentous injury: a summary of theories, evidence, and clinical interpretation. *Sports Med* 47: 1271–1288, 2017. doi:10.1007/s40279-016-0666-y.
55. **Kapreli E**, **Athanasopoulos S.** The anterior cruciate ligament deficiency as a model of brain plasticity. *Med Hypotheses* 67: 645–650, 2006. doi:10.1016/j.mehy.2006.01.063.